

SUBMITTED October 18, 2021

APPROVED March 10, 2022

PUBLISHED ONLINE March 23, 2022

PUBLISHED July 10, 2023

ASSOCIATE EDITOR
Manoel Barbosa Dantas

DOI: <http://dx.doi.org/10.18265/1517-0306a2021id6430>

ORIGINAL ARTICLE

Physical and mechanical properties of starch films: the role of the cross-linking mechanism through iodine binding capacity

 Aline Mercí ^[1]

 Mariana Moraes Góes ^{[2]*}

 Suzana Mali ^[3]

 Fabio Yamashita ^[4]

 Gizilene Maria de Carvalho ^[5]

[1] aline.merci@gmail.com

[2] marianagoes94@gmail.com

[5] gizilene@uel.br

Departamento de Química / Universidade Estadual de Londrina (UEL), Brazil

[2] smali@uel.br

Departamento de Bioquímica e Biotecnologia / Universidade Estadual de Londrina (UEL), Brazil

[4] fabioy@uel.br

Departamento de Ciência e Tecnologia de Alimentos / Universidade Estadual de Londrina (UEL), Brazil

ABSTRACT: In this study, a better knowledge of the influence of cross-linking mechanism on the mechanical properties of starch films is presented. Thus, waxy starch and cassava starch films, cross-linked with trisodium trimetaphosphate (STMP), were produced and characterized concerning their morphology, transport, and mechanical properties. Starch cross-linking was verified by RAMAN spectroscopy and by iodine binding capacity (IBC) values, which were determined by color analysis of digital images. Although cross-linking affects the morphology and crystallinity of the films, it was not observed a relationship between the mechanism of the cross-linking reaction of the starch chain (amylose-amylopectin and amylopectin-amylopectin) and the transport properties. The lower Young Modulus and IBC value and the higher elongation at break observed for cross-linking cassava starch films relative to control and waxy films indicate that cross-linking mechanism influences the mechanical properties of starch films and should be considered to tailor the final properties of packaging and biobased products.

Keywords: amylose content; cassava starch; chemical modification; mechanical properties; waxy maize starch.

Propriedades físicas e mecânicas dos filmes de amido: o papel do mecanismo de reticulação através da capacidade de ligação do iodo

RESUMO: Neste estudo, é apresentado um estudo da influência do mecanismo de reticulação nas propriedades mecânicas de filmes de amido. Assim, filmes de amido ceroso e de amido de mandioca, reticulados com trimetafosfato trissódico (TMPT), foram produzidos e caracterizados quanto à sua morfologia, transporte e propriedades mecânicas. A reticulação de amido foi verificada por espectroscopia RAMAN e por valores de capacidade de ligação de iodo (IBC),

*Corresponding author.

que foram determinados por análise de cor de imagens digitais. Embora a reticulação afete a morfologia e cristalinidade dos filmes, não foi observada relação entre o mecanismo de reação de reticulação da cadeia do amido (amilose-amilopectina e amilopectina-amilopectina) e as propriedades de transporte. O menor módulo de Young e valor de IBC e o maior alongamento na ruptura observado para filmes de amido de mandioca reticulados em relação aos filmes de controle e cerosos indicam que o mecanismo de reticulação influencia as propriedades mecânicas dos filmes de amido e deve ser considerado para adequar as propriedades finais de embalagens e produtos de base biológica.

Keywords: amido de mandioca; amido de milho ceroso; modificação química; propriedades mecânicas; teor de amilose.

1 Introduction

Starch has been considered one of the most promising materials in place of synthetic polymers due to its year-round availability, biodegradability, and low cost. One of the main advantages of using starch in packaging is its suitability to the technology already developed to produce synthetic materials, requiring a lower investment for film production. Brazil is the fourth largest cassava producer in the world (CONAB, 2020), which makes cassava starch a natural candidate for the development of new packaging materials. Although advantageous in terms of cost and environmental appeal, the films obtained are susceptible to moisture, resulting in changes in dimensional stability and mechanical properties. To overcome these problems, physical and chemical methods were used to develop starch-derived products, for example, blending with synthetic polymers and cross-linking reactions (CAGNIN *et al.*, 2021; DIYANA *et al.*, 2021; FORNACIARI *et al.*, 2020).

Cross-linking of different types of starches using multifunctional cross-linker agents to promote covalent inter and intramolecular bonding between hydroxyl groups of starch molecules is a well-established procedure (MASINA *et al.*, 2017). Trisodium trimetaphosphate (STMP) is among the most used cross-linker agents because it has low human toxicity (DONG; VASANTHAN, 2020; SUKHIJA; SINGH; RIAR, 2016). STMP cross-linked starches show higher crystallinity, solubility, permeability, and higher hydrophilicity than native starch films (BAGHERI *et al.*, 2019; GUTIÉRREZ *et al.*, 2015).

The mechanism of starch cross-linking reaction with STMP was studied by different authors and three mechanisms were described: reaction between amylose chains (AM–AM); reaction between amylopectin chains (AP–AP) and reaction between amylose and amylopectin chains (AM–AP). Numerous pieces of evidence had shown that amylose molecules do not crosslink to one another, but do crosslink to amylopectin chains (IMBERTY *et al.*, 1991; JANE *et al.*, 1999; KOU; GAO, 2019). Despite studies concerning the properties of cross-linked starches and the mechanisms of starch cross-linking reactions, consideration of cross-linking mechanism (AP–AP or AM–AP), and its relation to mechanical and transport properties in films of starch has been little explored.

This work aims to produce and characterize cross-linked cassava and waxy maize starch films and discuss the changes in the properties of the films considering the contribution of AP–AP and AM–AP mechanism of the cross-linking reaction using iodine

binding capacity (IBC). For this, it will be evaluated how the crosslinking mechanism influences the transport, mechanical and structural properties of the films produced. Therefore, this study is doubly convenient, as it evaluates properties of interest directly related to the cross-linking process and fills a gap in the literature.

2 Materials and methods

In this session, the techniques used for the production and characterization of starch films will be described.

2.1 Materials

Waxy maize starch (ADS, Matão-SP), cassava starch (YOKI, Paranaíba-PR), glycerol (Synth, Diadema-SP), Sodium Trimetaphosphate (STMP) (Sigma-Aldrich Chemistry, USA) and Amylose (Sigma-Aldrich, Lot # SLBQ8195V) were used in film production. Dimethyl sulfoxide (DMSO) was used to determine amylose content. Other reagents such as KI, sodium sulfate, hydrochloric acid (HCl), and sodium hydroxide (NaOH) were acquired from Synth, Brazil. All reagents were used as received.

2.2 Fabrication of the films

Starch films were prepared to employ 3 g of starch/100 g solution and glycerol (33 g/100 g of starch) as plasticizers (GÓES *et al.*, 2021). The mixture was heated to 95 °C for 40 minutes under constant stirring at 600 rpm (mechanical stirrer FISATON 713D) to obtain a film-forming solution. The filmogenic mixture was cooled at 30 °C and pH adjusted to 7.4 and then poured onto the acrylic plates to obtain control films (waxy maize control – WMC and cassava control – CAC).

Cross-linked films (waxy maize cross-linked – WMCL, and cassava cross-linked – CACL) were obtained by adding to the filmogenic mixture at 95 °C sodium sulfate and STMP (10% concerning dry starch) and keeping the agitation for 10 minutes. The filmogenic mixture was cold to 30 °C, with the pH adjusted to 9.5. The temperature of the solution was raised to 45 °C and the reaction continued for 2 hours with mechanical agitation at 600 rpm (mechanical stirrer FISATON 713D) and then poured onto the acrylic plates. The mixture was dried at 40 °C in a ventilated oven model TE-394-3 (Marconi N1040, Brazil) to constant weight (about 16 hours). The films produced were stored at 25 °C and relative humidity (RH) approximately 50%, until the characterization of these materials.

2.3 Amylose content

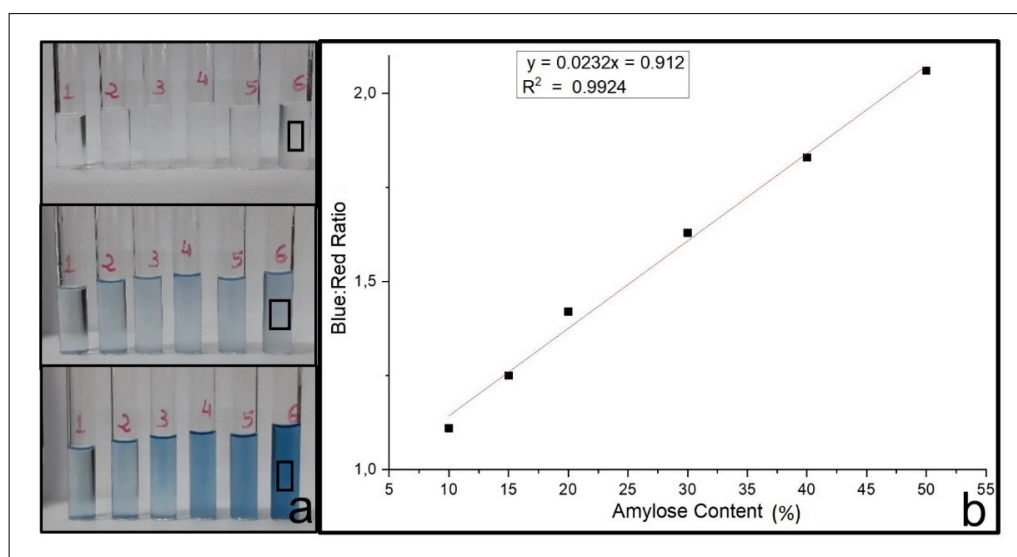
Determination of amylose content was performed as described by Hoover and Ratnayake (2001), with some modifications (4 mL of starch solution and 5 mL of KI / I₂ solution).

2.4 Image analysis Iodine Binding Capacity (IBC)

The IBC of control and cross-linked films was determined using digital images to quantify the blue color intensity after the reaction with iodine (KOU; GAO, 2019). Briefly, a standard curve for amylose/amylopectin proportions was obtained from amylose/amylopectin solutions and diluted to obtain concentrations of 0.010 g/L to 0.300 g/L of amylose. The solutions obtained were mixed vigorously with 1 mL of iodine solution (0.0025 M I₂/0.0065 M KI mixture) and allow developing color for 15 minutes (Figure 1a). A color JPEG image (150 dpi) of the solutions was obtained using a digital camera. Color analysis of the images (to obtain red, green, and blue component data) was performed using the commercial image analysis free program IMAGEJ (RASBAND, 1997). After the designation of an area within the image, the program returns a histogram and an average value of the red, green, and blue color components of the pixel within that area can be obtained. To consider both the increasing blue and decreasing red color, we decided to use the blue:red ratio for determining the amylose concentration. Graphing the ratio of blue:red intensities of each solution versus the amylose concentration gave a linear result (Figure 1b, $R^2 = 0.9924$). The blue:red (B:R) values of the films were determined by analyzing images obtained before and after 2 minutes by adding 1 drop of 0.0025 M I₂ / 0.0065 M KI solution to each film. All values indicated are averages of values obtained from two different replicates.

Figure 1 ▶

(a) Colorimetry of the starch-iodine reaction using a digital camera. Superior left: $t = 0$ minutes, middle left: $t = 1$ minute, inferior left: $t = 2$ minutes.
(b) Calibration curve of the blue:red ratio from the digital images at various amylose concentrations. This ratio provides a linear representation of amylose concentration.
Fonte: research data



2.5 Scanning Electron Microscopy (SEM)

The films (surface and cryofracture) were microscopically examined using a FEI Quanta 200 scanning electron microscope (Oregon, USA). The samples were covered with a thin layer of gold and the images were obtained using an acceleration voltage of 20 kV.

2.6 X-ray diffraction (XRD)

An X-ray diffractometer (PANalytical-X'Pert PRO MPD) was used to perform XRD studies. The voltage and current used were, respectively, 40 kV and 30 mA.

The 2θ scanning interval used varied from 2° to 120° with an angular pitch of 0.05° . The counting time per point was 2 s. To disregard possible preferential orientations in the sample preparation process, these samples were rotated cyclically during the measurement process over a period of 2 s.

The crystallinity index (CI) was determined from the deconvolution of the diffractogram (DOME *et al.*, 2020). The position and number of peaks were checked by the second derivative function of the original diffractograms. The ratio of the crystalline and amorphous area was determined from Equation 1.

$$CI = \frac{Ac}{Ac + Aa} \quad (1)$$

2.7 Raman spectroscopy

The Raman spectra of the films were obtained from a WITec Confocal Raman Equipment, System Alpha 300+. The excitation wavelengths were 532 nm and 785 nm. Raman images were adjusted using an objective lens with magnification of $100\times$ and spectra were recorded in different thicknesses of the sample with a 10 mm beam diameter and 10 minutes exposure.

2.8 Moisture adsorption kinetics

Starch film specimens ($20\text{ mm} \times 20\text{ mm}$) were pre-dried for 7 days over CaCl_2 and then were placed at 25°C over saturated salt solutions in separate desiccators having desired relative humidity (7%, 33%, 43%, 58%, 75%, and 83% RH) conditions (ROCKLAND, 1960). Weights of film specimens were measured as a function of time. The moisture content of the samples (M) was determined gravimetrically. Dry basis (d.b.) moisture content was used in calculations and data were fitted according to a mathematical model suggested by Peleg (1988), in Equation 2:

$$M_{(t)} = M_0 + \left(t / (k_1 + k_2 t) \right) \quad (2)$$

where: $M_{(t)}$ is the moisture after the test time; M_0 is the initial moisture content; t is the time measured in hours; k_1 is the Peleg velocity constant [$\text{h}/(\text{g water}/\text{g solids})$] and k_2 is the Peleg capacity constant ($\text{g solids}/\text{g of water}$). The parameters of the Peleg model were determined by non-linear regression. All tests were conducted in triplicate.

2.9 Sorption isotherms

The sorption isotherm curves were obtained from the data of moisture sorption kinetics after equilibrium was reached (equal weights after two consecutive measurements). Equilibrium moisture content was calculated from

the increase in mass of the dried sample after equilibration at a given RH. GAB (Guggenheim–Anderson–de Boer) model (Equation 3) was used to fit starch film sorption isotherm data (BIZOT; BULEON; RIOU, 1984).

$$X_w = \frac{(C \cdot K \cdot m_0 \cdot a_w)}{(1 - K \cdot a_w)} \times (1 - K \cdot a_w + C \cdot k \cdot a_w) \quad (3)$$

where: X_w is the moisture content of a given water activity (a_w); m_0 is the monolayer value g water/g solids; C and K are the GAB constants related to the interaction energy between the first layer of adsorbed molecules and the subsequent layers. All tests were conducted in triplicate.

2.10 Water vapor permeability (WVP)

The WVP of the films was determined by the method described in ASTM E 96-95 (ASTM, 1995) with some modifications. Each film sample was sealed over a circular opening (area = $2.8 \times 10^{-7} \text{ m}^2$) in a permeation cell that was conditioned at 25 °C in a desiccator. Anhydrous calcium chloride (0% RH) was placed inside the cell while the desiccator was kept at 75% RH. The change in the weight of the cell was measured at intervals of 2 hours between the 0–6 hours times and then every 24 hours over a week. The thickness of the films was determined at three different points of each sample, considering the film thickness as an average between all readings. The change in the weight of the cell was plotted as a function of time, and the slope of each line was calculated from linear regression. The water vapor permeation ratio (WVPR) was calculated from the slope (g/t) and the cell area (in m^2) using Equation 4:

$$WVP = \frac{\left(\frac{g}{t \times A}\right) \times e}{\Delta P} \quad (4)$$

where: g/t is the slope obtained by linear regression of mass gain (g) of the packaging versus time (s); A is the area (m^2) of permeation of each film; ΔP is the pressure difference (kPa) between the atmosphere containing calcium chloride and the distilled water-saturated environment, a value of 0.12 kPa; e is the thickness (m) of each film. All tests were carried out in triplicate.

2.11 Water solubility (%)

The film samples were cut into 2 cm × 2 cm specimens, dried in an air-circulating oven (Marconi-N1040) at 70 °C for 3 hours, and allowed to cool in a desiccator with silica gel. Then, the samples were placed in erlenmeyers with 50 mL of distilled water and closed with aluminum foil. The material was kept in an orbital shaker (Marconi-MA140 / CFT) at

25 °C at 180 rpm and after 24 hours the sample was collected and placed in an oven with air circulation for 24 hours at 60 °C and then cooled to 25 °C in a desiccator with silica gel, and after that, its final weight was noted. The solubility of the films in water (%) was calculated (GONTARD; GUILBERT; CUQ, 1992; RANGEL-MARRÓN *et al.*, 2019).

2.12 Mechanical tests

Ten film specimens (10 mm × 70 mm) of each formulation were pre-dried for 7 days over 58% RH. The tensile properties were determined using a TA.TX2i Stable Micro Systems texture analyzer (Surrey, England) by ASTM D-882-91 (ASTM, 1996). The parameters determined were tensile strength, TS (MPa), elongation at break, E (%), and Young's Modulus, YM (MPa).

3 Results and discussion

The produced starch films were characterized by IBC, structural, morphological, transport, and mechanical properties.

3.1 Amylose content and films production

The observed amylose contents for cassava and waxy starch, determined by IBC, from the calibration curve shown in Figure 1b, were $19.4 \pm 0.3\%$, and $0\% \pm 1\%$, respectively, and are within the values observed by other authors for cassava starch and waxy starch (16%–22% e 0%–2%, respectively) (VAN HUNG; PHI; VY, 2012). The films produced in this work, under the conditions analyzed (58% RH), were manageable and compact with no bubbles. Cross-linked starch films were thicker than control films ($1.5 \text{ mm} \pm 0.1 \text{ mm}$, $2.2 \text{ mm} \pm 0.1 \text{ mm}$, $1.7 \text{ mm} \pm 0.1 \text{ mm}$, and $1.9 \text{ mm} \pm 0.1 \text{ mm}$ for CAC, CACL, WMC, and WMCL, respectively).

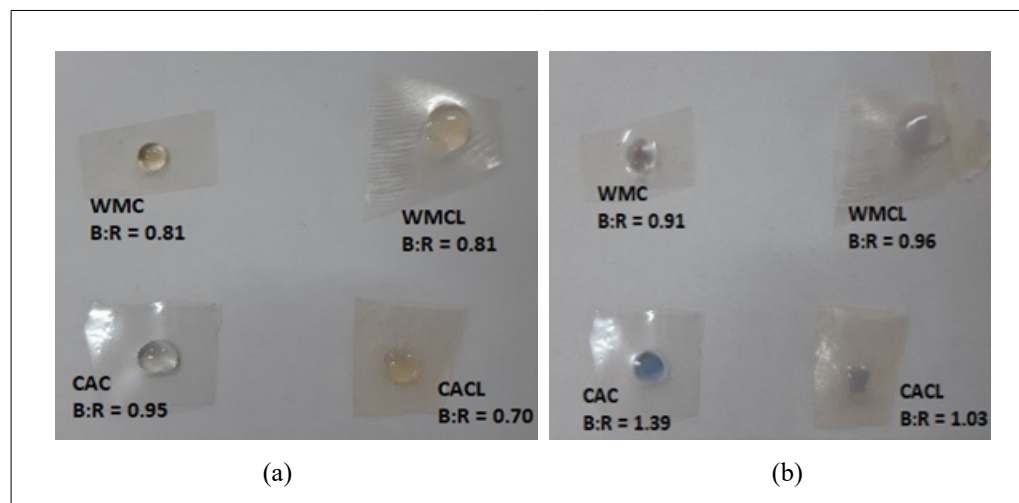
3.2 Image analysis Iodine Binding Capacity (IBC)

The starch cross-linking reaction with various reagents was evaluated by different authors. It is agreed that in the cross-linking process, the reaction occurs preferentially between amylose (AM) and amylopectin (AP), and AP–AP chains. The AM–AM reaction does not occur and cross-linking reaction between amylopectin molecules (AP–AP) is restricted to amorphous regions of amylopectin (JANE *et al.*, 1999; SHANNON; GARWOOD; BOYER, 2009; WOO; SEIB, 1997). After the cross-linking process the number of amylose molecules available to complex with iodine and the intensity of the blue color developed in the reaction decrease (KOU; GAO, 2019). Figure 2 shows the images from control and cross-linked starch films before and after 2 minutes of reaction with iodine. The reduction in amylose availability in CACL films compared to CAC films can be verified by reducing approximately 25% in the B:R ratio. This reduction in the B:R ratio value is equivalent to a reduction in amylose content, determined from Figure 1b, from 20.6% (CAC) to 5.2% (CACL). For the WMC and WMCL films, there was no variation in the B:R ratio. These results confirm that cross-linking reaction in cassava films occurs predominantly between AM with AP.

Figure 2 ▶

Images of control and cross-linked starch films (a) before and (b) after 2 minutes of reaction with iodine; the Blue:Red ratios (B:R) for each film were indicated.

Fonte: research data



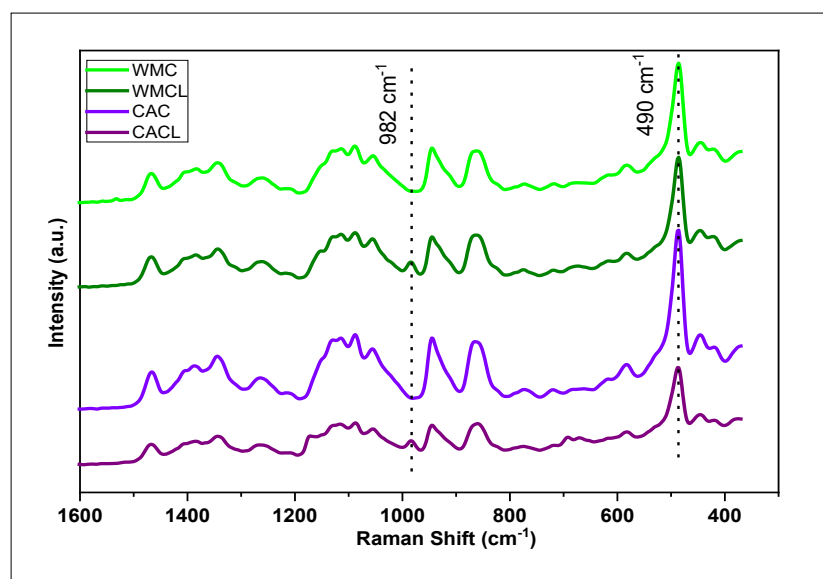
3.3 Raman spectroscopy

The Raman spectra of starch films in the range $400\text{--}2000\text{ cm}^{-1}$ were obtained and are similar despite the source and cross-linking reaction (Figure 3). The region below 700 cm^{-1} is the skeletal region of the molecule, which could be divided into two regions: $700\text{--}500\text{ cm}^{-1}$ region, called the "crystalline region", where the exocyclic deformations (OCC) are observed and the region range from 500 cm^{-1} to 450 cm^{-1} that has been attributed to endocyclic deformations (CCO, CCC) (MATHLOUTHI; KOENIG, 1987) as well as the C–O bond torsion and is correlated with different amylose contents (DANKAR *et al.*, 2018; YU *et al.*, 2018).

In Figure 3 it is observed that the band at 490 cm^{-1} decreases more sharply for CACL film than for WMCL film because of the reaction between amylose and amylopectin. This result agrees with what was verified by IBC. For the cross-linked films (WMCL and CACL) it is possible to observe a low-intensity band at 982 cm^{-1} attributed to the asymmetric vibration of elongation of the COP bonds (GARCÍA-TEJEDA *et al.*, 2016).

Figure 3 ▶

Raman spectra of starch films.
Fonte: research data



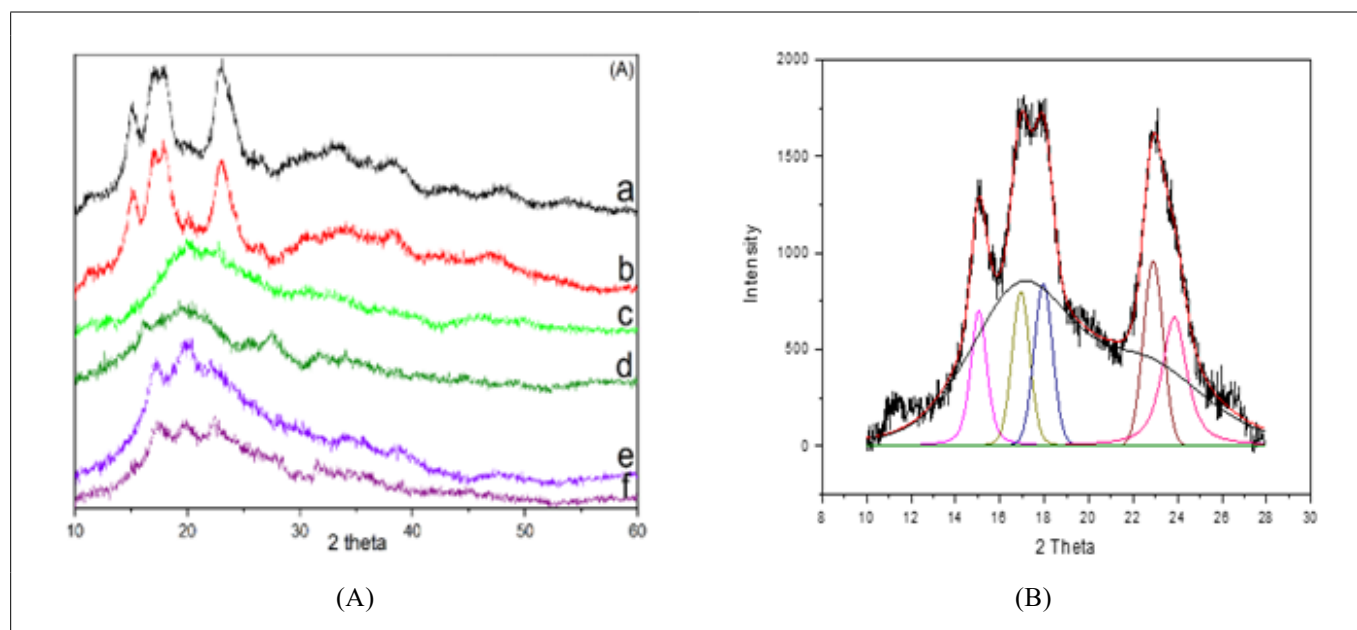
3.4 X-ray diffraction (XRD)

XRD diffractograms for native starches and films are shown in Figure 4(A). The crystalline Index (CI) of the starches and films was determined from the deconvoluted diffractograms and Figure 4(B) shows an example. The diffractograms of native starches show peaks at 15° and duet at 17.10° and 18.05° (Figure 4), characteristic of the type A polymorph. The CI determined were 31% and 33% for native cassava and native waxy maize starches, respectively. For the CAC and CACL films, only one crystalline peak was observed in 17.5° resulting in CI values of 6% and 3% respectively. The diffractogram of WMC and WMCL do not present these peaks.

Figure 4 ▼

(A): X-ray diffraction of:
 (a) Native waxy maize starch;
 (b) Native cassava starch;
 (c) Native waxy maize control film;
 (d) Waxy maize starch cross-linked film;
 (e) Cassava starch control film;
 (f) Cassava starch cross-linked film.
 (B): Deconvoluted diffractogram of native waxy maize, for determination of the crystallinity index (CI).
 Fonte: research data

On the other hand, there were characteristic peaks for the type B polymorph around 22° in CAC and CACL films, characterizing the transformation of polymorph A into polymorph type C (mixture of A and B) (SANTOS *et al.*, 2021). There are no reports in the literature about the transition from polymorph A to C in starch and glycerol film, to the best of the author's knowledge. The existence of crystalline peaks in the films may be due to the existence of a residual crystallinity or recrystallization of amylose and amylopectin. WMCL films show peaks around 16.22° and 28°, characteristic of amylopectin recrystallization (SUDHEESH *et al.*, 2021; VAN SOEST *et al.*, 1996). Despite the presence of these peaks, the amorphous pattern is dominant for WMC and WMCL films, resulting in an IC value of approximately zero.



The CAC and CACL films presented characteristic peaks polymorph V at 19.6°, possibly due to processing (temperature and stirring) (DOME *et al.*, 2020). Regarding the cross-linking of starch films, no characteristic peaks of the reagents used (STMP) were observed, indicating system homogeneity.

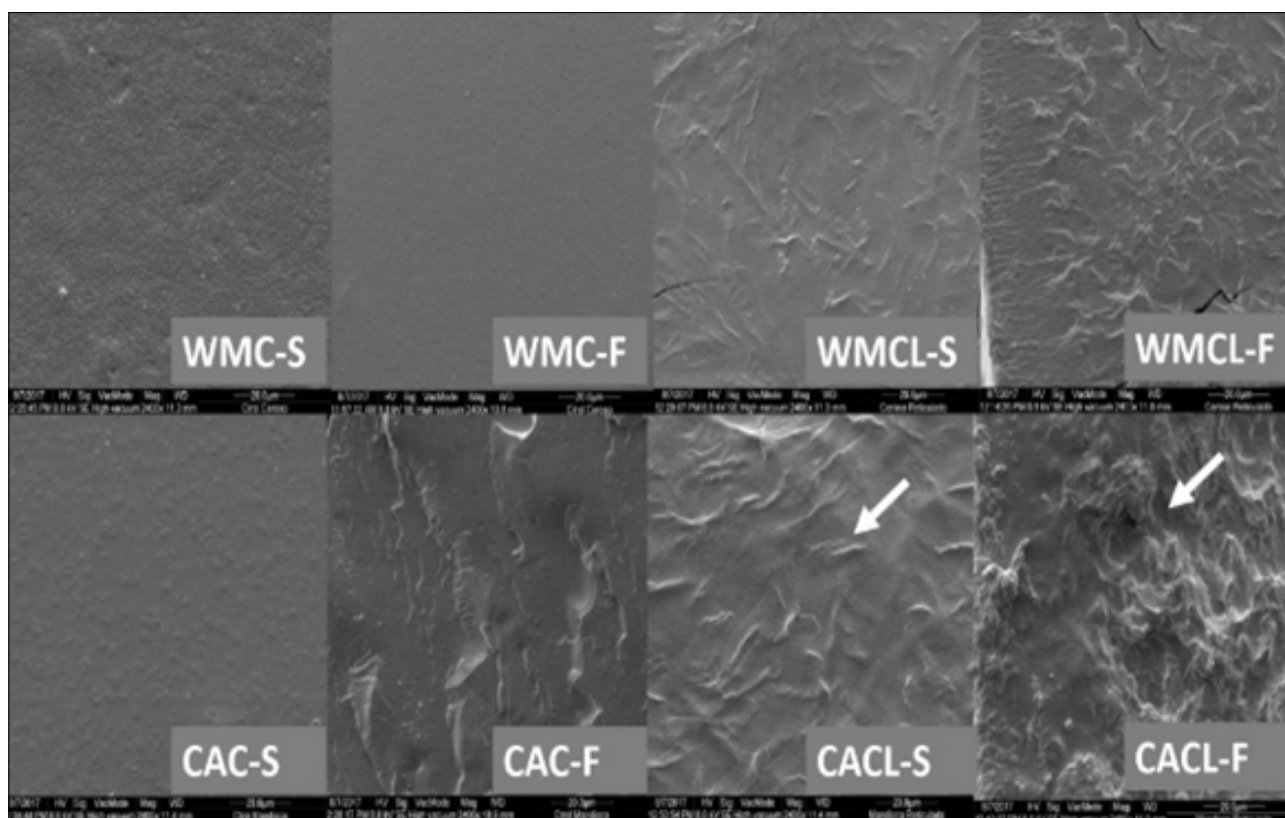
3.5 SEM

SEM images of the surface and cross-section of films are presented in Figure 5. Control films have a smoother and more homogeneous surface than crosslinked

Figure 5 ▼

SEM micrographs of films. S: images obtained for the surface at 2400× magnification: F: images obtained for film fracture at 2400× magnification.
Fonte: research data

films. In processing, plasticization transforms the granular morphology of starch into a homogeneous polymeric film, reducing intermolecular forces between polymer chains, and increasing their mobility and flexibility. The surface of the cross-linked films displays some structures (yellow arrow). These structures can be attributed to the inter-molecular ether and ester bonds that form between the STMP and the hydroxyl groups of the starch and glycerol molecule, which result in denser and more compact regions (OTHMAN *et al.*, 2019; SUDHEESH *et al.*, 2021; ZHOU *et al.*, 2015). The higher roughness present in the cross-section of the CACL films (white arrow) may be related to the nature and structure of cassava starch or even formed due to the free water contained in the sample, which was released after nitrogen fracture (ZHOU *et al.*, 2015).



3.6 Water vapor permeability (WVP) and water solubility (WS)

Water vapor permeability values of control and cross-linking films are shown in Table 1. The results indicate that the cross-linking process did not influence the WVP of the films (Tukey, $p \leq 0.05$).

Table 1 ►

WVP (0%-75% RH) and water solubility of control and cross-linked films.
Fonte: research data

Sample	WVP (10^{-10})(g.Pa ⁻¹ .s ⁻¹ .m ⁻¹)	Water Solubility (WS)(%)
WMC	1.13 ± 0.32 ^a	19.69 ± 2.17 ^c
WMCL	0.93 ± 0.28 ^a	31.89 ± 1.48 ^a
CAC	0.85 ± 0.41 ^a	18.71 ± 0.58 ^c
CACL	0.88 ± 0.59 ^a	29.44 ± 1.00 ^a

Mean ± standard deviation. Values in different letters in the same column indicate a significant difference between the samples (Tukey test. $p \leq 0.05$).

The films did not show physical disintegration after 24 hours of immersion in water at room temperature with gentle agitation. WS value for the cross-linked films was c.a. 30.0% (g/100 g dry film) corresponding mainly to the solubilized glycerol in water, which was added as a plasticizer at 33% (g/100 g dry film).

Analyzes of the physical properties indicate that the cross-linking process increases the solubility of starch films, as already observed by other authors (GUTIÉRREZ *et al.*, 2015). A reduction in solubility was expected, as the cross-linking reaction uses the hydrophilic sites of the polymer (OH groups) and introduces restriction to the mobility of the chains due to the generated three-dimensional structure. The increase in solubility observed may be an indication that part of the STMP may only be chemically modifying the starch, which contributes to the increase in the hydrophilicity of the films, favoring their solubilization. However, the mechanism of the cross-linking reaction amylose-amylopectin or amylopectin-amylopectin does not influence these properties.

3.7 Kinetics of water sorption

Water adsorption of starch films (data not shown) was more rapid at the initial times and lower amounts of water were adsorbed as time increased. Then the moisture content of starch films reached a plateau indicating that they achieved equilibrium with storage RH. Generally, films stored at high relative humidity conditions contained a higher amount of water compared to films stored at lower humidity conditions. Cross-linked films tend to absorb more water than control films.

The water content data obtained at specific times were fitted to the Peleg model and the data are presented in Table 2. It can be observed from Table 2, that the values of R^2 varied from 0.987 to 0.999 which confirmed the adequacy of the Peleg model in describing the water sorption behavior of starch films within the range of relative humidity. In general, k_1 and k_2 decreased with the increase in relative humidity. A low value of k_1 indicates that the films exhibit a high initial water sorption rate while a low value of k_2 indicates that the films exhibit high water adsorption capacity (MALI *et al.*, 2005; NAZREEN *et al.*, 2020). Meanwhile based on the results obtained in Table 2 it was found that cross-linked films exhibited lower k_1 and k_2 values at any RH compared to control films. This trend was due to the increase in the number of sites available for adsorption due to the increase in hydrophilicity and roughness in cross-linked films, as can be observed in SEM images (Figure 5). No difference was observed in the tendency of k_1 and k_2 variation for waxy starch and cassava films, indicating that the cross-linking mechanism does not interfere with the transport properties.

Table 2 ▼
Peleg model adjustment parameters ($M_{(t)}=M_0+(t/(k_1+k_2t))$) and the correlation coefficients.
Fonte: research data

Sample	43% RH				58% RH				75% RH			
	M_0	k_1	k_2	R^2	M_0	k_1	k_2	R^2	M_0	k_1	k_2	R^2
WMC	-0.001	72.687	11.621	0.995	-0.005	46.779	4.988	0.993	-0.002	41.198	4.375	0.992
WMCL	-0.002	95.806	10.327	0.991	-0.006	43.144	4.178	0.993	-0.004	40.175	3.660	0.987
CAC	0.001	203.912	12.055	0.999	0.000	51.961	4.768	0.992	-0.008	56.297	4.210	0.986
CACL	0.000	193.496	10.805	0.998	-0.007	51.027	4.554	0.989	-0.008	49.656	3.735	0.990

k_1 [h/(g water/g solids)] and k_2 (g solid / g water)

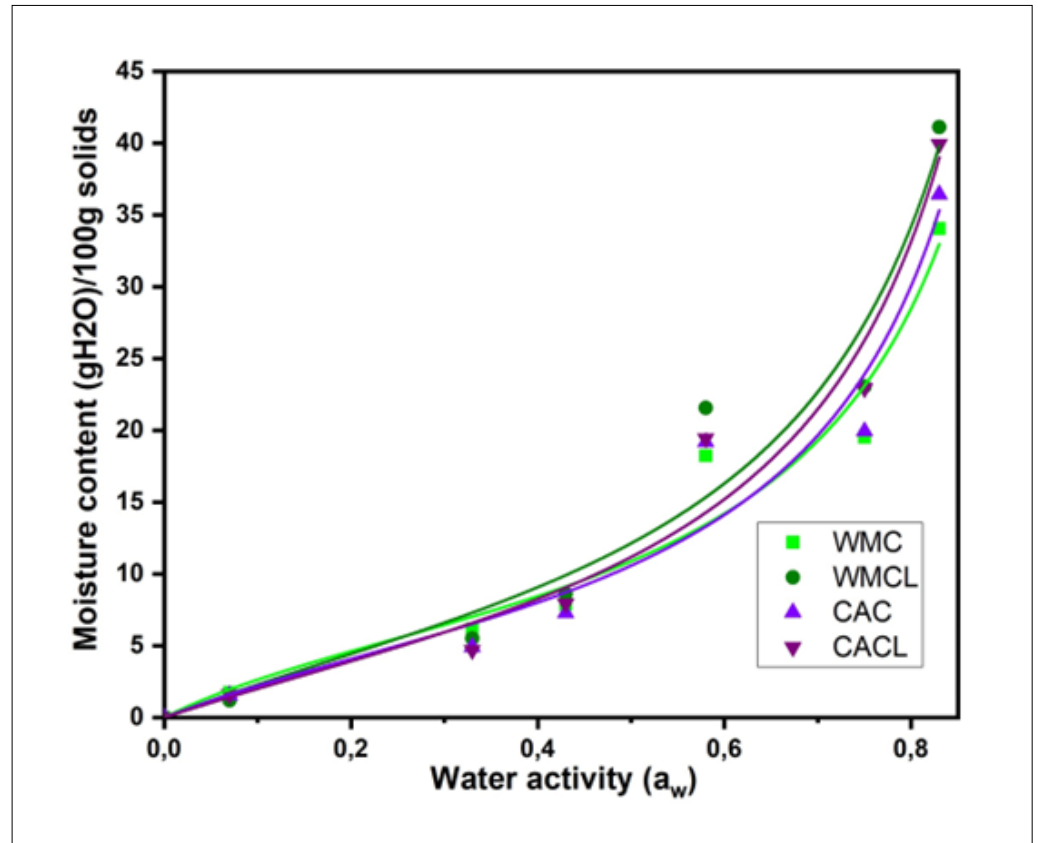
3.8 Water sorption isotherms

Water sorption data of starch films at different RH was fitted using the GAB model (Equation 3). The plot of moisture contents versus water activity (a_w) resulted in a sigmoid curve and the GAB model parameters was determined (Figure 6). In general, the more water activity, the higher the moisture contents (BAPTESTINI *et al.*, 2020; MALI *et al.*, 2005; MUSCAT *et al.*, 2013).

Figure 6 ►

Water sorption isotherm of films. The lines correspond to the values calculated by the GAB model.

Fonte: research data



At low water activities, the moisture content of the films increased slowly to 43%. This value on higher water activities implies a substantial water gain in the films. For low RH values, all films presented low equilibrium moisture contents (8 g water/g solids) and control films (waxy and cassava) presented higher values of equilibrium moisture contents than their respective cross-linked films. An inversion of this behavior occurs at 43% RH, and the cross-linked films have now higher equilibrium moisture content values than their respective controls. At 58% RH, the behavior of the films changes again, and the highest equilibrium moisture content values are observed for both cross-linked films.

The cross-linked films can be considered a two-phase system (OTHMAN *et al.*, 2019). Coexisting a mixture of highly cross-linked regions (dense) dispersed in the less cross-linked region. Because of this, some authors pointed out the structure of cross-linked films is heterogeneous. The dense structure of highly cross-linked regions is less likely to be penetrated by water reducing the values of M_0 . In the present study, the opposite effect was noticed and higher values of M_0 were observed in cross-linked films compared with control films. This was 6.831, 8.461, 6.852, 7.858 for the samples Waxy maize control; Waxy maize cross-linked;

Cassava control; Cassava cross-linked, respectively, findings that are consistent with those observed from the SEM (Figure 5), kinetics and solubility. In this case, we can suppose that the increase in the hydrophilicity in the crosslinked films prevails over the heterogeneity of the system.

The cross-linking reaction has the same effect on the M_0 values for both films, indicating that the mechanism (AM-AP or AP-AP) does not influence the water sorption capacity.

3.9 Mechanical properties

The effect of cross-linking on tensile strength (TS), Young Modulus (YM), and elongation at break (%E) of starch films are shown in Table 3. The results showed that cross-linking reaction has no influence on the mechanical properties of WMCL and resulted in CACL films with lower YM and TS and higher E (Tukey test. $p \leq 0.05$). Studies show that cross-linked starch improves the mechanical properties of starch films due to an increase in cross-linking density. Cross-linked starch molecules reinforce the intermolecular bond (covalent and hydrogen bonds) which increases the TS values. On the other hand, elongation at break is reduced for crosslinked starch films, a behavior attributed to the restriction of mobility of the crosslinked starch chains by diphosphate bonds (PREZZOTI *et al.*, 2012; SHARMA *et al.*, 2020).

Table 3 ▼
Mechanical properties of starch films.
Fonte: research data

Sample	Tensile Strength (TS) (MPa)	Elongation at break (E) (%)	Young's modulus (YM) (MPa)
WMC	3.39 ± 0.20 ^{b, c}	37 ± 2 ^b	32.8 ± 4.2 ^b
WMCL	3.38 ± 0.61 ^{b, c}	31 ± 2 ^b	36.8 ± 9.4 ^b
CAC	6.59 ± 1.08 ^a	43 ± 3 ^b	128.9 ± 28.9 ^a
CACL	2.08 ± 0.12 ^c	77 ± 6 ^a	34.5 ± 24.6 ^b

Mean ± standard deviation. Values in different letters in the same column indicate a significant difference between the samples (Tukey test. $p \leq 0.05$)

In this work, an opposite behavior was observed: cross-linking caused a reduction in TS and an increase in E. This behavior has been observed by other authors (REDDY; YANG, 2010; XU *et al.*, 2015) and attributed to the low concentrations of crosslinkers. At low concentrations, there is not enough cross-linking between the starch molecules to improve the tensile strength of the films (SILVA *et al.*, 2006). In our case, one possible explanation for this behavior is the increase in hydrophilicity observed by the solubility values, M_0 , $k1$, and $k2$ values of CACL and WMCL when compared to control films. However, the WMCL film also has greater hydrophilicity than the control film but does not have its mechanical properties altered. This observation leads us to suppose that another phenomenon should be considered. The two types of starch used in this work differ in the amylose content (AC): Cassava starch: 19% AC and Waxy Maize: 0% AC. We know that cross-linking reactions occur between AM-AP and AP-AP (JANE *et al.*, 1999). The use of STMP as a crosslinker causes two simultaneous effects: restriction in chain mobility and increases in hydrophilicity of films.

For WMCL films there is only the possibility of cross-linking by the AP-AP mechanism. Amylopectin chains already have mobility restrictions due to high molar mass and branches. Cross-linking between nearby chains within the same main

branch has more probability. Mobility restriction added by crosslink is fully offset by the plasticizing effect due to an increase in the hydrophilicity caused by the presence of phosphate groups and mechanical properties do not change.

AM–AP and AP–AP cross-linking mechanisms are equally probable in the CACL films since they occur in gelatinized starch (JANE *et al.*, 1999; KOU; GAO, 2019). The AP–AP mechanism has the same effect as in the WMCL film. The AM–AP cross-linking mechanism besides restricting the mobility of amylose chains and increasing hydrophilicity due to the presence of phosphate groups also contributes to an extra increase in hydrophilicity due to the alteration of amylose structure. The helical structure of amylose breaks down due to the cross-linking reaction, which can be verified by the lower B:R ratio value observed for CACL films. This extra effect makes the plasticization effect on CACL films overcome the effect of mobility restriction imposed by cross-linking, producing films with lower mechanical properties.

For the conditions analyzed in this work, it can be inferred that the cross-linking mechanism influences the mechanical properties of starch films and must be considered to modulate the final properties of the material. Careful analysis of the reaction conditions, types and amount of the cross-linking reagents and amylose content should be considered to achieve the desired effect on material properties.

4 Conclusions

Cross-linked films of cassava and waxy maize starch were successfully produced. The crosslinked films showed higher solubility, lower crystallinity, and roughness morphology when compared to control films. The lower values of k_1 , and k_2 indicate that crosslinked films exhibit a higher initial water sorption rate and higher water absorption capacity than control films, exhibiting greater hydrophilicity. This behavior can be attributed to the prevalence of contribution of the phosphate groups that are only grafted, which increases the mobility of the chains and the hydrophilicity of the films.

The IBC method can be used to infer the cross-linking reaction mechanism. At the level of phosphorous used, the cross-linking reaction between amylose/amylopectin is responsible for changes in the mechanical properties of cassava starch films. Cross-linking between AM–AP makes CACL more flexible and with lower tensile strength values than control and WMCL films. The cross-linking reaction between AP–AP does not change the mechanical properties of waxy maize films. In conclusion, we found that amylose content interferes with the cross-linking mechanism using STMP and with the mechanical properties of starch films. The choice of starch will depend on its end-use application.

Acknowledgment

We are grateful to the Spectroscopy Laboratory (ESPEC), Laboratory of Electronic Microscopy and Microanalysis (*LMEM*) and X-Ray Analysis Laboratory (LARX) – Multi-user Center of Research Laboratories (CMLP) of the State University of Londrina (UEL).

The authors would like to thank the Conselho Nacional de Desenvolvimento Científico e Tecnológico (CNPq – Brazil), Coordenação de Aperfeiçoamento de Pessoal de Nível Superior (CAPES – Brazil) and Fundação Araucária – Brazil for financial support.

Financing

This work was carried out with the support of the Coordination for the Improvement of Higher Education Personnel – Brazil (CAPES) – Financing Code 001.

Conflict of interest

The authors declare no conflicts of interest associated with this work.

References

ASTM – AMERICAN SOCIETY FOR TESTING AND MATERIALS. **Standard test method for water vapor transmission of material. E96-95**. Philadelphia: ASTM, 1995.

ASTM – AMERICAN SOCIETY FOR TESTING AND MATERIALS. **Standard test method for tensile properties of thin plastic sheeting. D882-91**. Philadelphia: ASTM, 1996.

BAGHERI, V.; GHANBARZADEH, B.; AYASEH, A.; OSTADRAHIMI, A.; EHSANI, A.; ALIZADEH-SANI, M.; ADUN, P. A. The optimization of physico-mechanical properties of bionanocomposite films based on gluten/ carboxymethyl cellulose/ cellulose nanofiber using response surface methodology. **Polymer Testing**, v. 78, 105989, 2019. DOI: <https://doi.org/10.1016/j.polymertesting.2019.105989>.

BAPTESTINI, F. M.; CORRÊA, P. C.; RAMOS, A. M.; JUNQUEIRA, M. S.; ZAIDAN, I. R. GAB model and the thermodynamic properties of moisture sorption in soursop fruit powder. **Revista Ciência Agronômica**, v. 51, n. 1, e20164781, 2020. Available at: <http://periodicos.ufc.br/revistacienciaagronomica/article/view/88787/242157>. Accessed on: 9 Aug. 2023.

BIZOT, H.; BULEON, A.; RIOU, N. Study of native starch hydration: influence of sorption hysteresis. **Journal de Physique Colloques**, v. 45, n. C7, p. C7-259-C7-264, 1984. DOI: <https://doi.org/10.1051/jphyscol:1984730>.

CAGNIN, C.; SIMÕES, B. M.; YAMASHITA, F.; CARVALHO, G. M.; GROSSMANN, M. V. E. pH sensitive phosphate crosslinked films of starch-carboxymethyl cellulose. **Polymer Engineering & Science**, v. 61, n. 2, p. 388-396, 2021. DOI: <https://doi.org/10.1002/pen.25582>.

CONAB – COMPANHIA NACIONAL DE ABASTECIMENTO (CONAB). **Análise mensal**. Mandioca: fevereiro de 2020. Brasília, DF: CONAB, 2020. Available at: <https://www.conab.gov.br/info-agro/analises-do-mercado-agropecuario-e-extrativista/analises-do-mercado/historico-mensal-de->

[mandioca/item/download/31054_7353a3a223023f519813432dd4ef8c25](https://doi.org/10.1016/j.foodchem.2018.03.138).

Accessed on: 21 Aug. 2020. In Portuguese.

DANKAR, I.; HADDARAH, A.; OMAR, F. E. L.; PUJOLÀ, M.; SEPULCRE, F. Characterization of food additive-potato starch complexes by FTIR and x-ray diffraction. **Food Chemistry**, v. 260, p. 7-12, 2018. DOI: <https://doi.org/10.1016/j.foodchem.2018.03.138>.

DIYANA, Z. N.; JUMAIDIN, R.; SELAMAT, M. Z.; GHAZALI, I.; JULMOHAMMAD, N.; HUDA, N.; ILYAS, R. A. Physical properties of thermoplastic starch derived from natural resources and its blends: a review. **Polymers**, v. 13, n. 9, p. 1396, 2021. DOI: <https://doi.org/10.3390/polym13091396>.

DOME, K.; PODGORBUNSKIKH, E.; BYCHKOV, A.; LOMOVSKY, O. Changes in the crystallinity degree of starch having different types of crystal structure after mechanical pretreatment. **Polymers**, v. 12, n. 3, p. 641, 2020. DOI: <https://doi.org/10.3390/polym12030641>.

DONG, H.; VASANTHAN, T. Effect of phosphorylation techniques on structural, thermal, and pasting properties of pulse starches in comparison with corn starch. **Food Hydrocolloids**, v. 109, 106078, 2020. DOI: <https://doi.org/10.1016/j.foodhyd.2020.106078>.

FORNACIARI, B.; BERNARDINO, B. L.; GÓES, M. M.; CARVALHO, G. M. Filmes de amido reticulado: estudo da incorporação e liberação de sulfato de condroitina / Crosslinked- starch films: study of the incorporation and release of chondroitin sulfate. **Brazilian Journal of Development**, v. 6, n. 7, p. 51298-51309, 2020. DOI: <https://doi.org/10.34117/bjdv6n7-684>.

GARCÍA-TEJEDA, Y. V.; SALINAS-MORENO, Y.; HERNÁNDEZ-MARTÍNEZ, Á. R.; MARTÍNEZ-BUSTOS, F. Encapsulation of purple maize anthocyanins in phosphorylated starch by spray drying. **Cereal Chemistry**, v. 93, n. 2, p. 130-137, 2016. DOI: <https://doi.org/10.1094/CCHEM-04-15-0072-R>.

GÓES, M. M.; MERCI, A.; ANDRELLO, A. C.; YAMASHITA, F.; CARVALHO, G. M. Design and application of multi-layer Starch-Latex blends as phosphorous delivery system. **Journal of Polymers and the Environment**, v. 29, p. 2000-2012, 2021. DOI: <https://doi.org/10.1007/s10924-020-02018-w>.

GONTARD, N.; GUILBERT, S.; CUQ, J.-L. Edible wheat gluten films: influence of the main process variables on film properties using response surface methodology. **Journal of Food Science**, v. 57, n. 1, p. 190-195, 1992. DOI: <https://doi.org/10.1111/j.1365-2621.1992.tb05453.x>.

GUTIÉRREZ, T. J.; MORALES, N. J.; PÉREZ, E.; TAPIA, M. S.; FAMÁ, L. Physico-chemical properties of edible films derived from native and phosphated cush-cush yam and cassava starches. **Food Packaging and Shelf Life**, v. 3, p. 1-8, 2015. DOI: <https://doi.org/10.1016/j.fpsl.2014.09.002>.

HOOVER, R.; RATNAYAKE, W. S. Determination of total amylose content. **Current Protocols in Food Analytical Chemistry**, v. 00, n. 1, p. E2.3.1-E2.3, 2001. DOI: <https://doi.org/10.1002/0471142913.fae0203s00>.

IMBERTY, A.; BULÉON, A.; TRAN, V.; PÉEREZ, S. Recent advances in knowledge of starch structure. **Starch-Stärke**, v. 43, n. 10, p. 375-384, 1991. DOI: <https://doi.org/10.1002/star.19910431002>.

JANE, J.; CHEN, Y. Y.; LEE, L. F.; MCPHERSON, A. E.; WONG, K. S.; RADOSAVLJEVIC, M.; KASEMSUWAN, T. Effects of amylopectin branch chain length and amylose content on the gelatinization and pasting properties of starch. **Cereal Chemistry**, v. 76, n. 5, p. 629-637, 1999. DOI: <https://doi.org/10.1094/CCHEM.1999.76.5.629>.

KOU, T.; GAO, Q. A study on the thermal stability of amylose-amylopectin and amylopectin-amylopectin in cross-linked starches through iodine binding capacity. **Food Hydrocolloids**, v. 88, p. 86-91, 2019. DOI: <https://doi.org/10.1016/j.foodhyd.2018.09.028>.

MALI, S.; GROSSMANN, M. V. E.; GARCÍA, M. A.; MARTINO, M. N.; ZARITZKY, N. E. Mechanical and thermal properties of yam starch films. **Food Hydrocolloids**, v. 19, n. 1, p. 157-164, 2005. DOI: <https://doi.org/10.1016/j.foodhyd.2004.05.002>.

MASINA, N.; CHOONARA, Y. E.; KUMAR, P.; TOIT, L. C.; GOVENDER, M.; INDERMUN, S.; PILLAY, V. A review of the chemical modification techniques of starch. **Carbohydrate polymers**, v. 157, p. 1226-1236, 2017. DOI: <https://doi.org/10.1016/j.carbpol.2016.09.094>.

MATHLOUTHI, M.; KOENIG, J. L. Vibrational spectra of carbohydrates. **Advances in Carbohydrate Chemistry and Biochemistry**, v. 44, p. 7-89, 1987. DOI: [https://doi.org/10.1016/S0065-2318\(08\)60077-3](https://doi.org/10.1016/S0065-2318(08)60077-3).

MUSCAT, D.; ADHIKARI, R.; MCKNIGHT, S.; GUO, Q.; ADHIKARI, B. The physicochemical characteristics and hydrophobicity of high amylose starch-glycerol films in the presence of three natural waxes. **Journal of Food Engineering**, v. 119, n. 2, p. 205-219, 2013. DOI: <https://doi.org/10.1016/j.jfoodeng.2013.05.033>.

NAZREEN, A. Z.; JAI, J.; ALI, S. A.; MANSOR, N. M. Moisture adsorption isotherm model for edible food film packaging: a review. **Scientific Research Journal**, v. 17, n. 2, p. 222-245, 2020. DOI: <https://doi.org/10.24191/srj.v17i2.10160>.

OTHMAN, S. H.; KECHIK, N. R. A.; SHAPI'I, R. A.; TALIB, R. A.; TAWAKKAL, I. S. M. A. Water sorption and mechanical properties of starch/chitosan nanoparticle films. **Journal of Nanomaterials**, v. 2019, 3843949, 2019. DOI: <https://doi.org/10.1155/2019/3843949>.

PELEG, M. An empirical model for the description of moisture sorption curves. **Journal of Food Science**, v. 53, n. 4, p. 1216-1217, 1988. DOI: <https://doi.org/10.1111/j.1365-2621.1988.tb13565.x>.

PREZOTTI, F. G.; MENEGUIN, A. B.; EVANGELISTA, R. C.; CURY, B. S. F. Preparation and characterization of free films of high amylose/pectin mixtures cross-linked with sodium trimetaphosphate. **Drug Development and Industrial Pharmacy**, v. 38, n. 11, p. 1354-1359, 2012. DOI: <https://doi.org/10.3109/03639045.2011.650863>.

RANGEL-MARRÓN, M.; MANI-LÓPEZ, E.; PALOU, E.; LÓPEZ-MALO, A. Effects of alginate-glycerol-citric acid concentrations on selected physical, mechanical, and barrier properties of papaya puree-based edible films and coatings, as evaluated by response surface methodology. *LWT*, v. 101, p. 83-91, 2019. DOI: <https://doi.org/10.1016/j.lwt.2018.11.005>.

RASBAND, W. S. **ImageJ**: Image processing and analysis in Java. Bethesda, USA: U. S. National Institutes of Health, 1997. Available at: <https://imagej.nih.gov/ij/>. Accessed on: 15 Mar. 2022.

REDDY, N.; YANG, Y. Citric acid cross-linking of starch films. *Food Chemistry*, v. 118, n. 3, p. 702-711, 2010. DOI: <https://doi.org/10.1016/j.foodchem.2009.05.050>.

ROCKLAND, L. B. Saturated salt solutions for static control of relative humidity between 5° and 40° C. *Analytical Chemistry*, v. 32, n. 10, p. 1375-1376, 1960. DOI: <https://doi.org/10.1021/ac60166a055>.

SANTOS, T. B.; CARVALHO, C. W. P.; OLIVEIRA, L. A.; OLIVEIRA, E. J.; VILLAS-BOAS, F.; FRANCO, C. M. L.; CHÁVEZ, D. W. H. Functionality of cassava genotypes for waxy starch. *Pesquisa Agropecuária Brasileira*, v. 56, e02414, 2021. DOI: <https://doi.org/10.1590/S1678-3921.pab2021.v56.02414>.

SHANNON, J. C.; GARWOOD, D. L.; BOYER, C. D. Genetics and physiology of starch development. In: BEMILLER, J.; WHISTLER, R. (ed.) **Starch: Chemistry and Technology**. 3. ed. Academic Press, 2009. chapter 3, p. 23-82. DOI: <https://doi.org/10.1016/B978-0-12-746275-2.00003-3>.

SHARMA, V.; KAUR, M.; SANDHU, K. S.; GODARA, S. K. Effect of cross-linking on physico-chemical, thermal, pasting, *in vitro* digestibility and film forming properties of Faba bean (*Vicia faba* L.) starch. *International Journal of Biological Macromolecules*, v. 159, p. 243-249, 2020. DOI: <https://doi.org/10.1016/j.ijbiomac.2020.05.014>.

SILVA, M. C.; IBEZIM, E. C.; RIBEIRO, T. A. A.; CARVALHO, C. W. P.; ANDRADE, C. T. Reactive processing and mechanical properties of cross-linked maize starch. *Industrial Crops and Products*, v. 24, n. 1, p. 46-51, 2006. DOI: <http://doi.org/10.1016/j.indcrop.2006.01.001>.

SUDHEESH, C.; SUNOOJ, K. V.; JAMSHEER, V.; SABU, S.; SASIDHARAN, A.; AALIYA, B.; NAVAF, M.; AKHILA, P. P.; GEORGE, J. Development of bioplastic films from γ - irradiated kithul (*Caryota urens*) starch; morphological, crystalline, barrier, and mechanical characterization. *Starch-Stärke*, v. 73, n. 5-6, 2000135, 2021. DOI: <https://doi.org/10.1002/star.202000135>.

SUKHIJA, S.; SINGH, S.; RIAR, C. S. Effect of oxidation, cross-linking and dual modification on physicochemical, crystallinity, morphological, pasting and thermal characteristics of elephant foot yam (*Amorphophallus paeoniifolius*) starch. *Food Hydrocolloids*, v. 55, p. 56-64, 2016. DOI: <https://doi.org/10.1016/j.foodhyd.2015.11.003>.

VAN HUNG, P.; PHI, N. T. L.; VY, T. T. V. Effect of debranching and storage condition on crystallinity and functional properties of cassava and potato starches. *Starch/ Stärke*, v. 64, n. 12, p. 964-971, 2012. DOI: <https://doi.org/10.1002/star.201200039>.

VAN SOEST, J. J. G.; HULLEMAN, S. H. D.; WIT, D.; VLIEGENTHART, J. F. G. Crystallinity in starch bioplastics. **Industrial Crops and Products**, v. 5, n. 1, p. 11-22, 1996. DOI: [https://doi.org/10.1016/0926-6690\(95\)00048-8](https://doi.org/10.1016/0926-6690(95)00048-8).

WOO, K.; SEIB, P. A. Cross-linking of wheat starch and hydroxypropylated wheat starch in alkaline slurry with sodium trimetaphosphate. **Carbohydrate Polymer**, v. 33, n. 4, p. 263-271, 1997. [https://doi.org/10.1016/S0144-8617\(97\)00037-4](https://doi.org/10.1016/S0144-8617(97)00037-4).

XU, H.; CANISAG, H.; MU, B.; YANG, Y. Robust and flexible films from 100% starch cross-linked by biobased disaccharide derivative. **ACS Sustainable Chemistry & Engineering**, v. 3, n. 11, p. 2631-2639, 2015. DOI: <https://doi.org/10.1021/acssuschemeng.5b00353>.

YU, Z.; WANG, Y.-S.; CHEN, H.-H.; LI, Q.-Q.; WANG, Q. The gelatinization and retrogradation properties of wheat starch with the addition of stearic acid and sodium alginate. **Food Hydrocolloids**, v. 81, p. 77-86, 2018. DOI: <https://doi.org/10.1016/j.foodhyd.2018.02.041>.

ZHOU, W.; YANG, J.; HONG, Y.; LIU, G.; ZHENG, J.; GU, Z.; ZHANG, P. Impact of amylose content on starch physicochemical properties in transgenic sweet potato. **Carbohydrate Polymers**, v. 122, p. 417-427, 2015. DOI: <https://doi.org/10.1016/j.carbpol.2014.11.003>.